A SCLEROCHRONOLOGICAL ANALYSIS ON THE MEDITERRANEAN BIVALVE *OSTREA EDULIS* (LINNAEUS, 1758): A QUICK AGE DETERMINATION METHOD

MAURO PIETRO NEGRI & CESARE CORSELLI

Università degli Studi di Milano Bicocca, Piazza della Scienza 4, I-20126 Milan, Italy

Abstract *Valves of the ostreid bivalve* Ostrea edulis *(Linnaeus, 1758) were analyzed by visual sclerochronology based on umbonal ridges and internal growth lines, along with the calcitic chalky lenses deposited below the adductor muscle scars. The lenses are herein proposed for the first time as a tool for a quick age determination. The analysis revealed ages of 5 to 7.5 years, consistent with shells' dimensions. A Von Bertalanffy growth curve, markedly different from published analogous ones, showed that shell height alone is not a valid proxy for age determination. The adopted sclerochronological method is advised for age assessment of oyster settlement on human artifacts on the seafloor.*

Key words *Sclerochronology*, Ostrea edulis, *chalky lenses, Von Bertalanffy.*

INTRODUCTION

Visual sclerochronological analyses performed on ostreid bivalves generally aim to identify visible growth traces in the internal structure of sectioned valves. These traces result from differential growth rate (Walne, 1958), maximum during the warm half-year (from mid-spring to early autumn) and minimum – or definitely stopped – during the cold one (from mid-autumn to early spring). This annual cycle depends on both thermal and trophic variations over the year. The winter growth stop leads to the formation (usually at the end of the period) of lighter or more frequently darker lines or bands among shell layers; sometimes, a superimposed detachment of calcitic layers takes place along these discontinuities. The annual bands are deposited throughout the whole shell, being more clearly visible in the umbonal-ligamental area (Milner, 2001; Richardson, Collis, Ekaratne, Dare & Key, 1993); they are often hardly distinguishable elsewhere in the valve, since they are frequently hidden by cavitations (i.e. demineralization caused by other organisms) and/or irregular growth of specimens. Yearly growth lines originate from variation in density of daily ones (Clausen, 1974). Also, the differential seasonal growth rate creates, in the ligamental pit, a yearly alternation of concavities and convexities (i.e. shallow furrows and ridges), related to maximum summer and minimum winter growth rates, respectively (Kirby, Soniat & Spero, 1998; Milner, 2001). In addition to these commonly used morphological features, in the present paper an innovative analysis of internal "chalky" calcite deposits is proposed. These deposits were hitherto described in malacological papers only in terms of functional morphology (Chinzei, 1986, 1995; Kirby, 2001; Komatsu, Chinzei, Zakhera & Matsuoka, 2002; MacDonald, Freer & Cusack, 2010): oysters create such lenticular bodies by quickly depositing calcite blades or flakes, either randomly or in definite zones of the valve; the deposited structure retains a large amount of void space, thus being considerably lighter than the "normal" microcrystalline calcite of the shell. Supposedly, the presence of chalky lenses reduces the weight of the valves, improves their resistance to shocks and predation, smoothers the internal surface, and provides the mollusc with a quickly adjustable body support. Nevertheless, their exact role remains unclear (Dauphin, Ball, Castillo-Michel, Chevallard, Cuif, Farre, Pouvreau & Salomé, 2013).

A common methodology for visual sclerochronological examination comprises the longitudinal sectioning of valves from the umbo to the ventral margin (Marchitto, Jones, Goodfriend & Weidman, 2000; Milner, 2001; Richardson *et al*., 1993), i.e. along the maximum growth direction, and the analysis of shell structures visible on the obtained polished sections, with the aid of acetate peels or thin sectioning if necessary (cf. Toland, Perkins, Pearce, Keenar & Leng, 2000).

Since *Ostrea edulis* is not a particularly long-lived species, it is unsuitable for usually recognized

Contact author : mauro.negri2@unimib.it

long-term sclerochronological applications (i.e. palaeoenvironmental and palaeoclimatic reconstructions); conversely, the proposed analysis could address the needs of age assessment of recent submerged human artifacts, by stating the time they became "available" to oysters settling.

Materials and Methods

Between June and September 2009, six samples (L0-L5) of shell material were recovered off Livorno harbor, in the Northern Tyrrhenian Sea (Central Italy), at about 40–50m depth (Fig. 1). The sampling was carried out during two SCUBA diving sessions on the same small bottom area, characterized by a widespread shell growth on small hard substrates.

All samples yielded live bivalve specimens belonging to the family Ostreidae Rafinesque, 1815, and in particular to the species *Ostrea edulis* (Linnaeus, 1758) and *Crassostrea virginica* (Gmelin, 1791). All specimens had settled and grown on a metallic substrate, presumably iron, and coming from scrap or wrecks deposited on the sea floor.

All samples were washed at the paleontological laboratory of Milano-Bicocca University, then dried under an extractor fan and subsequently treated for 24h in a 3% solution of H_2O_2in order to remove organic matter and allow the valves to open. Three samples out of six (namely L0, L2 and L3) were selected for the sclerochronological analysis, since they yielded fully grown specimens of *O. edulis* (L. 1758). Two specimens (L0A and L0B) were selected from sample L0, and their valves labeled L0A', L0A", L0B' and L0B" (with ' and " denoting valves from the same specimen); one of these latter (L0B") subsequently proved to be useless for the analysis, owing to the presence in it of extensive cavitations completely hiding the internal structure. Two specimens (L2A and L2B) were selected from sample L2 (valves labeled L2A', L2B' and L2B"), while a single specimen (L3A) was selected from sample L3 (valve labeled L3A').

Figure 1 Map showing the sampling location in the Northern Tyrrhenian Sea (black star). Base map by Hans Braxmeier (www.maps-for-free.com).

All selected valves were sectioned along the maximum growth direction (i.e. longitudinally, from the umbo to the ventral margin) by means of 24mm cutting discs on a Ferm Combitool FCT-400F manual grinder; the two half-valves obtained from each valve were labeled *r* and *l* ("right" and "left") with reference to their position relative to the longitudinal axis of the shell (in external view). All half-valves were then cleaned and polished by means of professional sandpaper of decreasing grain (dry scraping with P240, P400, P600, P1000 and P1500 grains; wet scraping with P2000 grain).

The polished sections were then visually analyzed under an optical stereomicroscope with up to 40 X magnification, and photographed with an HP Photosmart 812 4.13 megapixel digital camera mounted on the microscope.

The maximum shell height (Tab. 1) was measured from the umbo to the ventral margin, excluding the fragile peripheral prismatic layers in order to obtain comparable values; this measure matches the "nacreous shell height" *sensu* Milner (2001).

The growth curve (Fig. 2), plotting age versus (nacreous) shell height, is based on the Von Bertalanffy growth equation

$$L_t=L_\infty[1-e^{-K\,(t-t_0)}]$$

where L=shell height, t=age, L_∞=maximum theoretical (asymptotic) shell height, K=constant with units of reciprocal time, and t_0=age corresponding to zero height. In the present case, t_0 was assumed to be=0 due to the very small (negligible) dimensions of oyster spats.

The curve parameters K and L_∞ were estimated by means of Gulland & Holt plot plus a linear regression (cf. Sparre & Venema, 1998). Input data for the plot (Tab. 2) were the ages (t) obtained from sclerochronological analysis and the mean nacreous shell heights (L) for each age. Secondary values in Tab. 2 are $\Delta t=t_i - t_{i-1}$, $DL=L(t_i) - L(t_{i-1})$,

Table 1 Summary of the characters of all valves selected for the sclerochronological analysis. Italic denotes secondary features. Identifiers (ID.) as in 'Materials and methods' section.

Sample (ID.)	Valve (ID.)	Shell height (mm)	Observable features	Estimated age	Figures
L0	L0A' (right)	82	ligamental ridges *growth lines*	6.5 years	4A-D
	L0A'' (left)	82	ligamental ridges *growth lines*	7.5 years	4E-H
	L0B' (left)	80	ligamental ridges growth lines chalky lenses	6.5 years	5A-F
L2	L2A' (right)	71	*ligamental ridges* growth lines	5.5 years	6A-D
	L2B' (right)	66	*ligamental ridges* *growth lines* chalky lenses	5 years	6E-L
	L2B'' (left)	68	ligamental ridges *growth lines* chalky lenses	6 years	7A-F
L3	L3A' (right)	67	ligamental ridges *growth lines* chalky lenses	5 years	8A-F

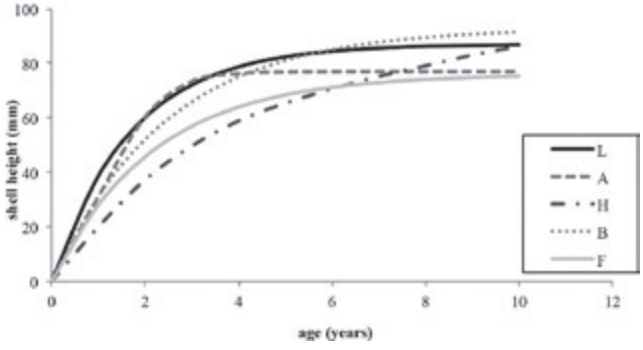

Figure 2 Von Bertalanffy growth curve based on age/length data, compared with those discussed in the 'Discussion' section. Abbreviations: L, Livorno (present study); A, Adriatic Sea (Fabi *et al*., 1989); H, Hampshire (Rodhouse, 1978); B, Blackwater River (Richardson *et al*., 1993); F, Fal/Solent River (Richardson *et al*., 1993).

Table 2 Input data for the construction of the Gulland & Holt plot. See 'Materials and methods' section for symbols.

t	Δt	L	DL	L'	DL/Δt
5		66.5			
5.5	0.5	71	4.5	68.75	9
6.5	1	81	10	76	10
7.5	1	82	1	81.5	1

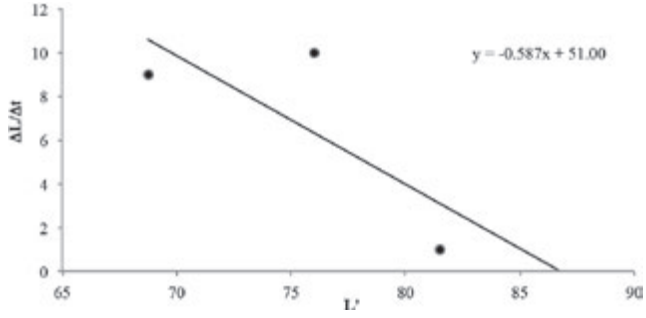

Figure 3 Gulland & Holt plot based on age/length data. The equation for the linear regression line is reported in the graph. See 'Materials and methods' section for symbols.

and $L'=(L(t_i)+L(t_{i-1}))/2$. The graph of Fig. 3 plots L' versus DL/Δt. The relatively small Δt values obtained from base data justify the use of Gulland and Holt plot (Sparre & Venema, 1998). The equation for the regression line is y=-0.587x +51.00; accordingly, obtained values to fit Von Bertalanffy equation are K=(-×coefficient)=0.587, and L_∞=regression line intercept on×axis=87.

RESULTS

The results of the visual analysis of all half-valves are summarized in Table 1. The following

sections report on the observations made on each single half-valve.

Valve L0A' (Figs 4A, B).

Half-valve L0A'*r* (Fig. 4C). In the weakly curved ligamental area six annual ridges (indicated by white arrows on the section) are observed, the oldest (apical) one less visible. The protuberances between ridges 3/4 and 4/5 are minor thickenings, not corresponding to ligamental ridges. Each ridge seems to match in the section with a light growth line, that corresponding to ridge 2 partially hidden by an internal cavitation (ca). The line path appears slightly upward concave at first, then convex right of the dark vertical band visible in the middle of the section; this convexity is also highlighted by the calcite layer detachment on the right. The last (= youngest) ligamental concavity, just below ridge 6, is very short, well agreeing with the early summer sampling of the specimen. An age of 6.5 years can then be inferred.

Half-valve L0A'*l* (Fig. 4D). Observable features are nearly exactly the same as for L0A'*r*, but for a wider area hidden by the cavitation, placed more marginally and opened towards the ligamental area.

Valve L0A" (Figs 4E, F).

Half-valve L0A"*r* (Fig. 4G). Six annual ridges are observed in the ligamental pit, each corresponding to an evident protuberance in the section (white arrows); a minor thickening, not representing a ridge, is observable between ridges 3 and 4. Each ridge matches with a light growth band, the oldest one (starting at ridge 1) partially hidden by a cavitation (ca); the bands run almost flat at first, then approach one another and become convex, following the valve morphology. The abrupt color variation visible just right of ridge 6, following a dome-shaped path, is the result of a subsequent breakage. As in the previously described valve, the youngest concavity (below ridge 6) is very short, since the specimen was harvested at the beginning of summer. It is of note that the breaking/erosion of the apical part, above ridge 1, may have removed the shell material corresponding to a further yearly cycle. This should agree with the considerable (82mm) height of the valve, standing as the biggest one in the examined lot. Accordingly, the estimated age is 7.5 years.

Half-valve L0A"*l* (Fig. 4H). Observable features are similar to those of L0A"*r*; nevertheless, the obliquely-directed apical erosion removed much more shell material on this side of the valve, including ridge 1. Only five ligamental ridges (2–6) can thus be observed, and the "false ridge" is once again detectable between ridges 3 and 4. Also the light growth bands are less visible in the section.

Valve L0B' (Figs 5A, B).

Half-valve L0B'*r* (Figs 5C, E). Annual ligamental ridges originate barely evident protuberances in the umbonal section of this valve (white arrows and numbers in Fig. 5C). Ridges 1 and 2 are very close one another, and placed at some distance from the apex, while other ridges are more regularly spaced through the ligamental pit. Secondary bumps, not linked to ridges, are visible between ridges 2 and 3. As in the previously described valves from the same sample, shell material deposited after the youngest ridge is scarce. Each ridge match in the section with hardly visible growth lines (marked by black arrows and numbers), following an upward convex path at first and then becoming more or less straight. Four lines (2, 4, 5 and 6) are clearly revealed by superimposed detachments between the calcitic layers, leaving wide cavitations in the valve structure. The mid section (Fig. 5E) shows six chalky lenses in the area immediately below the adductor muscle scar; the dorso-ventral extension of each lens is defined by the black vertical arrows. Relatively thick crystalline calcitic layers separate the lenses; thinner layers often subdivide the main lenses into smaller ones, though not extending from the internal to the external margin of the shell. A clear example is provided by lens 3: within the main chalky body, thin calcitic veils define two secondary lenses, one on the left (extended from the internal cavity to mid-shell) and one on the right (placed towards the external side of the valve). It is of note that the small lenses (el) visible above lens 1 are not comprised in age calculation, since they belong to the external layers of the shell and do not relate with muscle scars. Taking into account all the morphological evidences, an age of 6.5 years is inferred for the specimen at hand.

Half-valve L0B'*l* (Figs 5D, F). Visible features are exactly the same as for L0B'*r*; ligamental ridges (Fig. 5D) are even less evident on this side

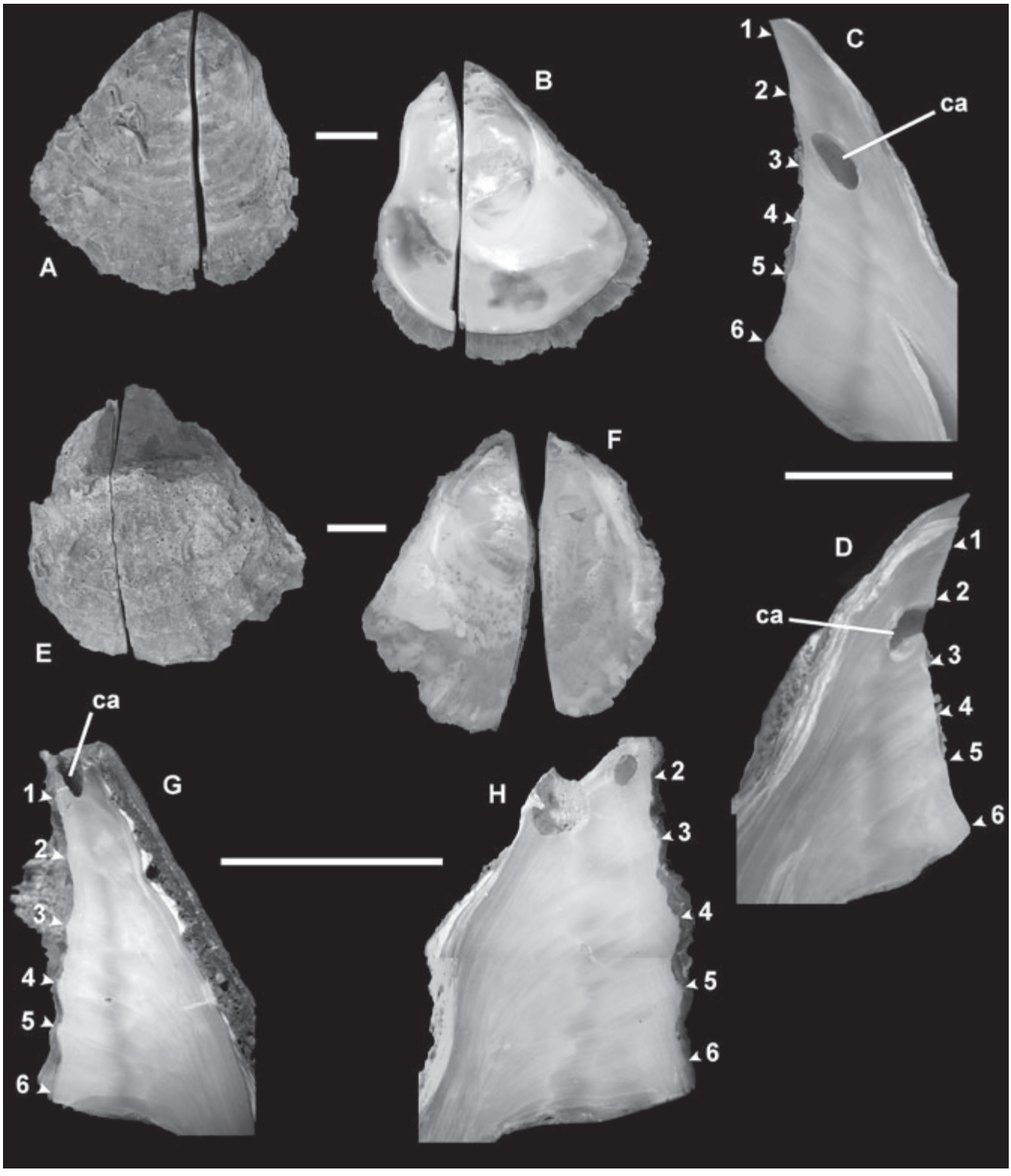

Figure 4A–B Valve L0A', external (A) and internal (B) views, sectioned in two half-valves. **C–D**. Half-valves L0A'*r* (C) and L0A'*l* (D), umbonal section; numbers/arrows mark the position of annual ligamental ridges. **E–F**. Valve L0A'', external (E) and internal (F) views, sectioned in two half-valves. **G–H**. Half-valves L0A''*r* (G) and L0A''*l* (H), umbonal section; numbers/arrows mark the position of annual ligamental ridges. Abbreviations: ca, cavitation. Scale bars: **A–B, E–F**=20.0mm; **C–D, G–H**=5.0mm.

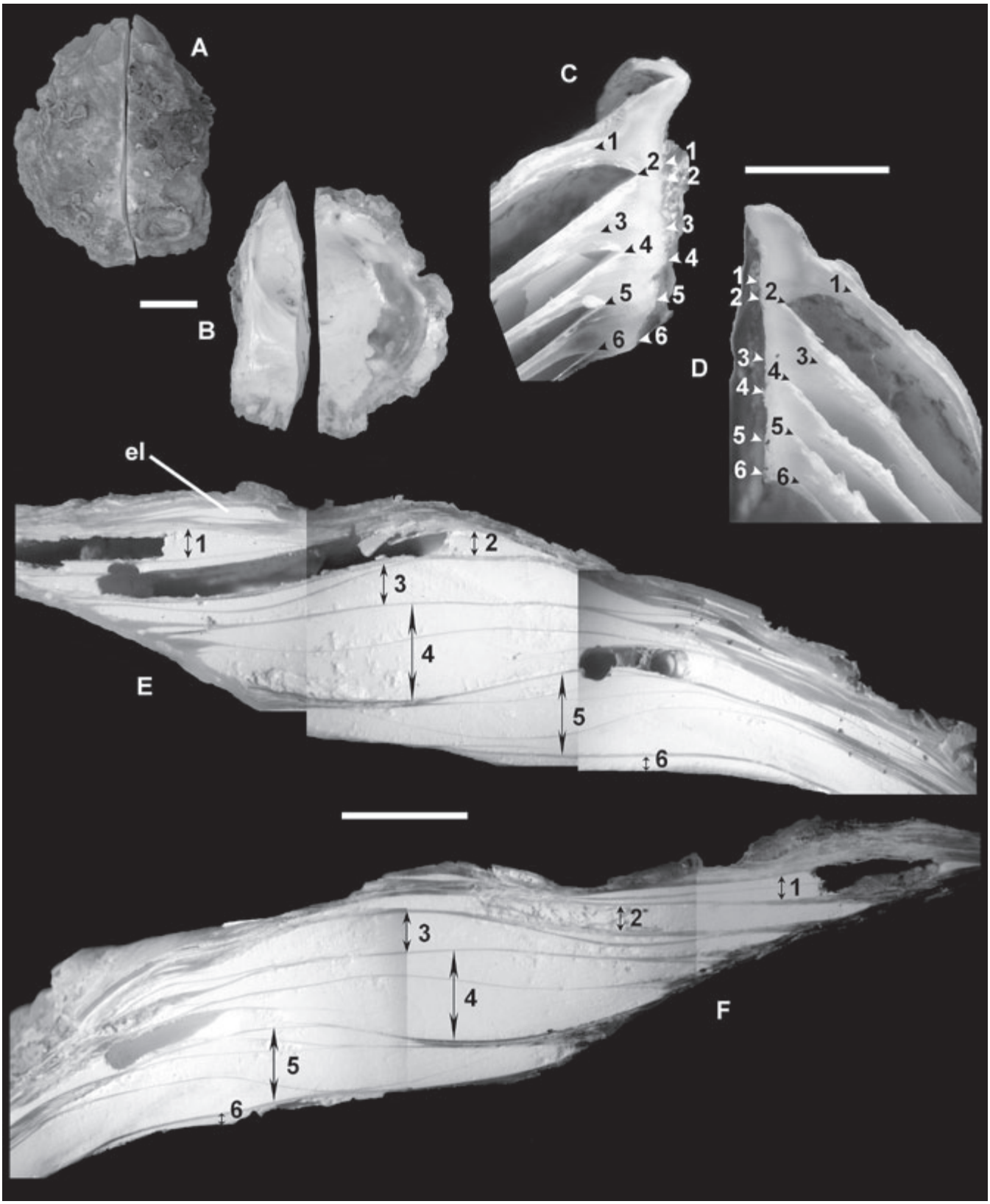

Figure 5A–B Valve L0B', external (A) and internal (B) views, sectioned in two half-valves. **C-D**. Half-valves L0B'*r* (C) and L0B'*l* (D), umbonal section; white numbers/arrows mark the position of annual ligamental ridges, black numbers/arrows that of corresponding growth lines/calcitic detachments. **E-F**. Half-valves L0B'*r* (E) and L0B'*l* (F), mid section; black numbers/arrows mark annual chalky lenses below the muscle scar area. Abbreviations: el, external lenses. Scale bars: **A–B**=20.0mm; **C–F**=5.0mm.

of the valve, where the ligamental pit is nearly flattened.

VALVE L2A' (Figs 6A, B).

Half-valve L2A'*r* (Fig. 6C). In this case, annual ligamental ridges are ill-defined on the ligamental pit, and corresponding protuberances (white arrows and numbers) are scarcely visible in the section. Ridges 1 and 2 (extremely thin) are placed near the apex and very close one another; other ridges are somewhat more protruding and regularly spaced. Each ridge matches with a growth line (black arrows), very faint at first, then becoming more evident where calcitic layers show initial steps of detachment; here, they appear as dark bands, or more properly as abrupt color changes from darker to lighter areas. Some other color variations are visible in between, but they do not match with any ligamental ridge. Line 1 is partially hidden by a cavitation (ca), while line 5 is marked by an irregular deposition of calcitic layers (ir). The inferred age of this specimen is 5.5 years.

Half-valve L2A'*l* (Fig. 6D). This half-valve doesn't exhibit substantial differences from L2A'*r*; line 1 is somewhat more evident, and an additional cavitation occurs between lines 2 and 3.

VALVE L2B' (Figs 6E, F).

Half-valve L2B'*r* (Figs 6G, I). The umbonal area (Fig. 6G) of this specimen is of no use at all. Only 4 undefined ligamental ridges were counted, really hardly detectable in the section (white arrows), apart from ridge 1. Growth lines are confused; only three faint slightly darker bands (black arrows) are hardly distinguishable quite far from the ligamental margin, and cannot be related to the ridges. Conversely, the mid section (Fig. 6I) is much more significant. Five chalky lenses are observable beneath the muscle scar area, their relatively small dimension being merely a consequence of a cutting path slightly apart from the maximum extension zone. In this case, only lens 5 shows a secondary, thin calcitic layer subdividing it into smaller lenses. Lens 5 (the youngest one) is completely formed, i.e. bordered towards the inner side of the valve by a crystalline calcitic lamina (cl); this well agrees with the specimen collection in late September, when annual growth is in slowdown phase. The inferred age is of at least 5 years, consistent with the relatively smaller size of the shell (66mm).

Half-valve L2B'*l* (Figs 6H, L). Both umbonal and mid sections appear to be strictly similar to those of L2B'*r*. The ligamental ridges (white arrows in Fig. 6H) appear higher in the section because of the strongly oblique growth of the umbonal area. Small secondary lenses (Fig. 6L) are noted also at the bottom of lens 3 and at the top of lens 4.

VALVE L2B" (Figs 7A, B).

Half-valve L2B"*r* (Figs 7D, E). Also in this case the umbonal area (Fig. 7D) is scarcely significant. Six low annual ridges occur on the ligamental pit, but they are ill-defined at the margin of the section (white arrows), except for ridges 5 and 6. Once more, growth lines are very confused, and only two – corresponding to faint dark bands (black arrows) – can be detected, apparently following a sinuous path. Conversely, in the mid section (Fig. 7E) six chalky lenses are observed below the adductor scar area. They are delimited by thick crystalline layers, and very few (and extremely thin) secondary layers occur within lenses 3 and 4; lens 5 appears extensively bioeroded. As for L2B' valve, the youngest lens (i.e. lens 6) is completely formed, as expected in a specimen sampled at the beginning of autumn. It is of note that the numerous, stacked small lenses (el) visible in the upper left corner of Fig. 7E are not related to the muscle scar and belong to the external layers of the shell. Accordingly, the inferred age of this specimen is 6 years.

Half-valve L2B"*l* (Figs 7C, F). There are no substantial differences with half-valve L2B"*r*. In the umbonal section (Fig. 7C), the different spacing of the six ridges (with respect to L2B"*r*) is due to the irregular growth of the ligamental area. The low fold between ridges 4 and 5 derives from a splitting of ridge 4. The mid section (Fig. 7F) appears to be less complete, lens 1 being only partially visible and lens 2 considerably smaller than its L2B"*r* counterpart. This is mainly due to the angular cutting path aiming to intercept both umbonal area and maximum extension zone of the chalky lenses.

VALVE L3A' (Figs 8A, B).

Half-valve L3A'*r* (Figs 8C, E). Annual ridges are not well defined on the ligamental pit. In the umbonal section of this half-valve (Fig. 8C) only three low folds are recognizable on the mid-lower

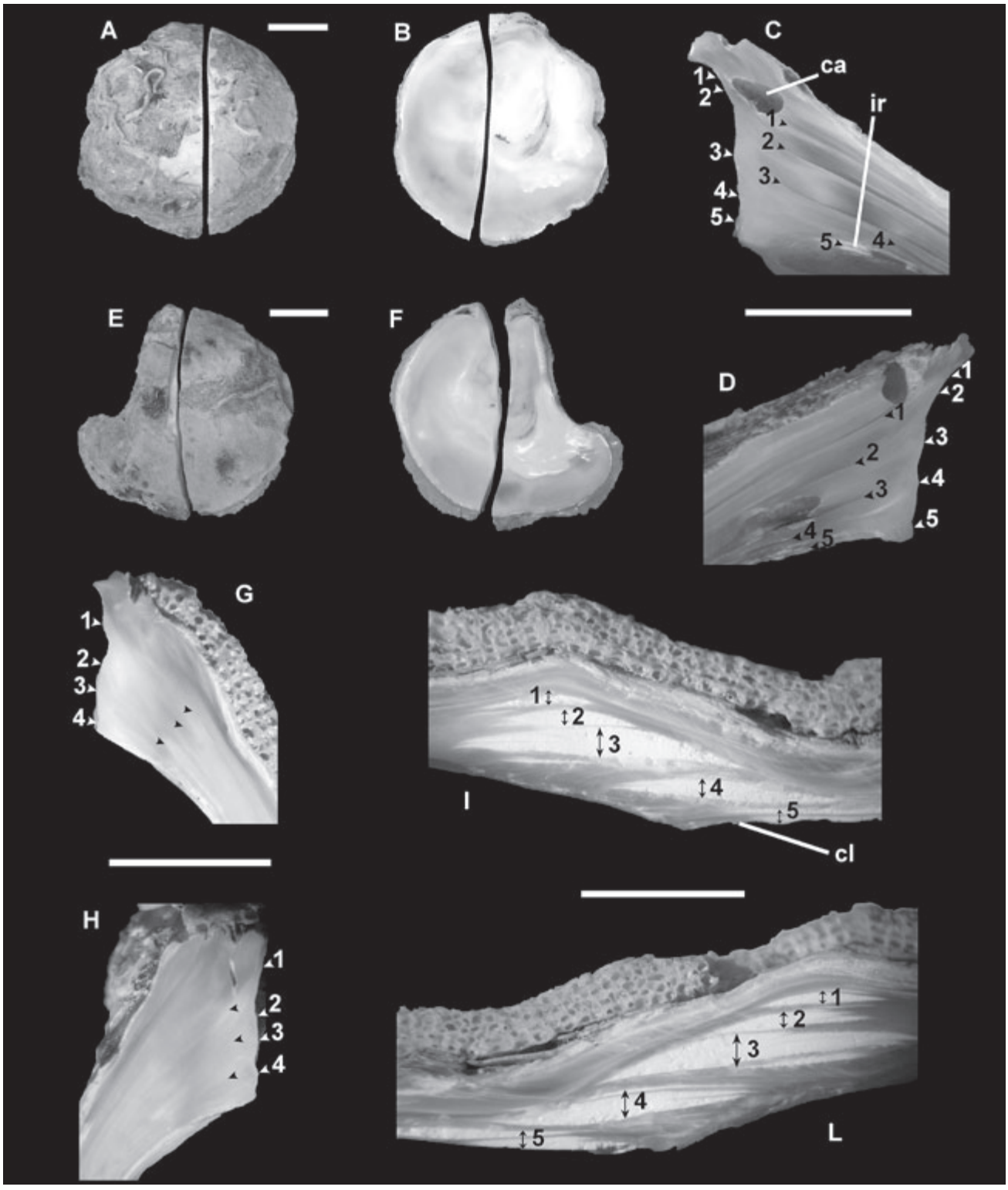

Figure 6A–B Valve L2A', external (A) and internal (B) views, sectioned in two half-valves. **C–D**. Half-valves L2A'*r* (C) and L2A'*l* (D), umbonal section; white numbers/arrows mark the position of annual ligamental ridges, black numbers/arrows that of corresponding growth lines/calcitic detachments. **E–F**. Valve L2B', external (E) and internal (F) views, sectioned in two half-valves. **G–H**. Half-valves L2B'*r* (G) and L2B'*l* (H), umbonal section; white numbers/arrows mark the position of annual ligamental ridges, black arrows that of some growth lines. **I–L**. Half-valves L2B'*r* (I) and L2B'*l* (L), mid section; black numbers/arrows mark annual chalky lenses below the muscle scar area. Abbreviations: ca, cavitation; ir, irregular calcite deposition; cl, crystalline calcitic layer. Scale bars: **A–B, E–F**=20.0mm; **C–D, G–L**=5.0mm.

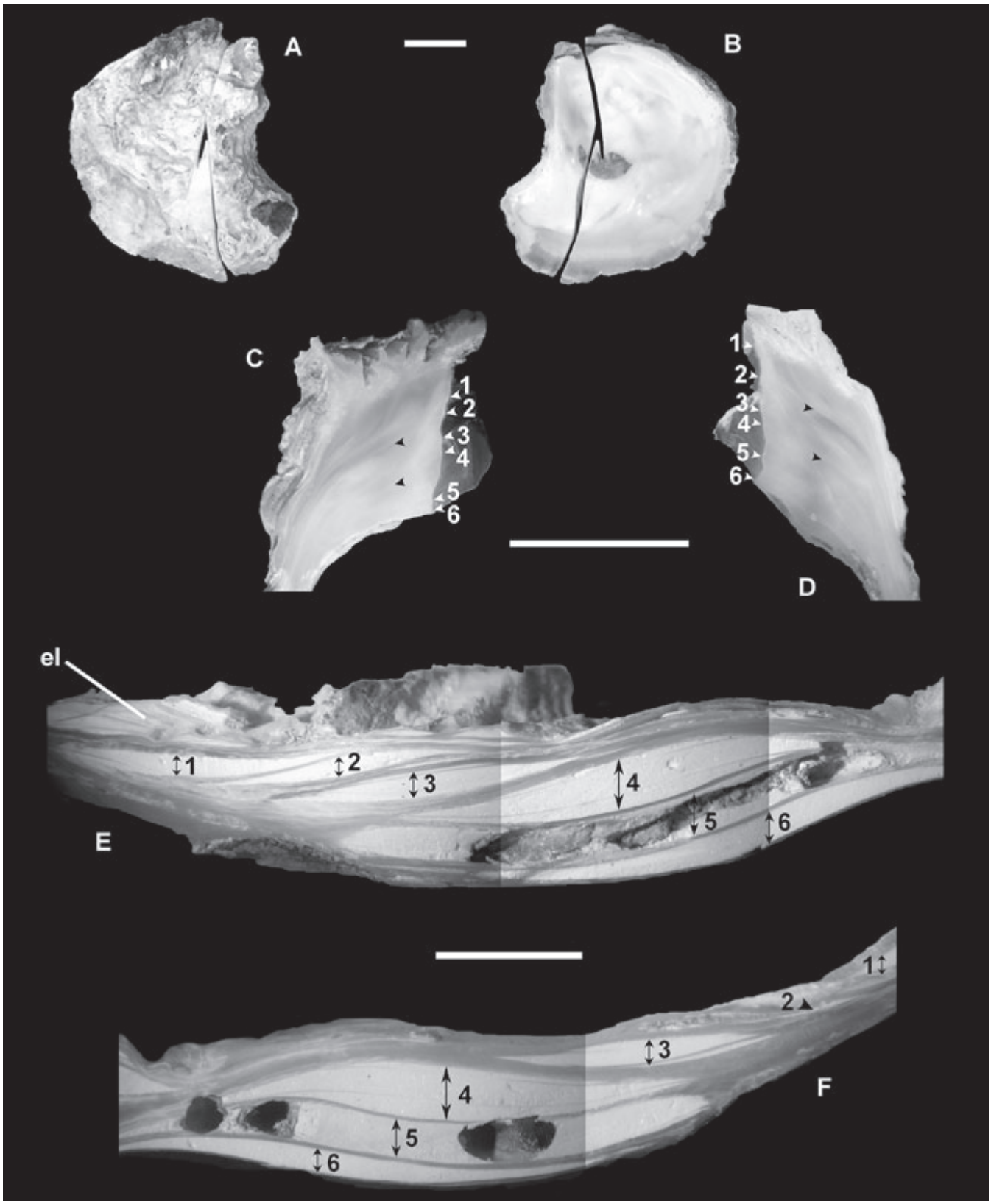

Figure 7A–B Valve L2B", external (A) and internal (B) views, sectioned in two half-valves. **C–D**. Half-valves L2B"*r* (D) and L2B"*l* (C), umbonal section; white numbers/arrows mark the position of annual ligamental ridges, black arrows that of some growth lines. **E–F**. Half-valves L2B"*r* (E) and L2B"*l* (F), mid section; black numbers/arrows mark annual chalky lenses below the muscle scar area. Abbreviations: el, external lenses. Scale bars: **A–B**=20.0mm; **C–F**=5.0mm.

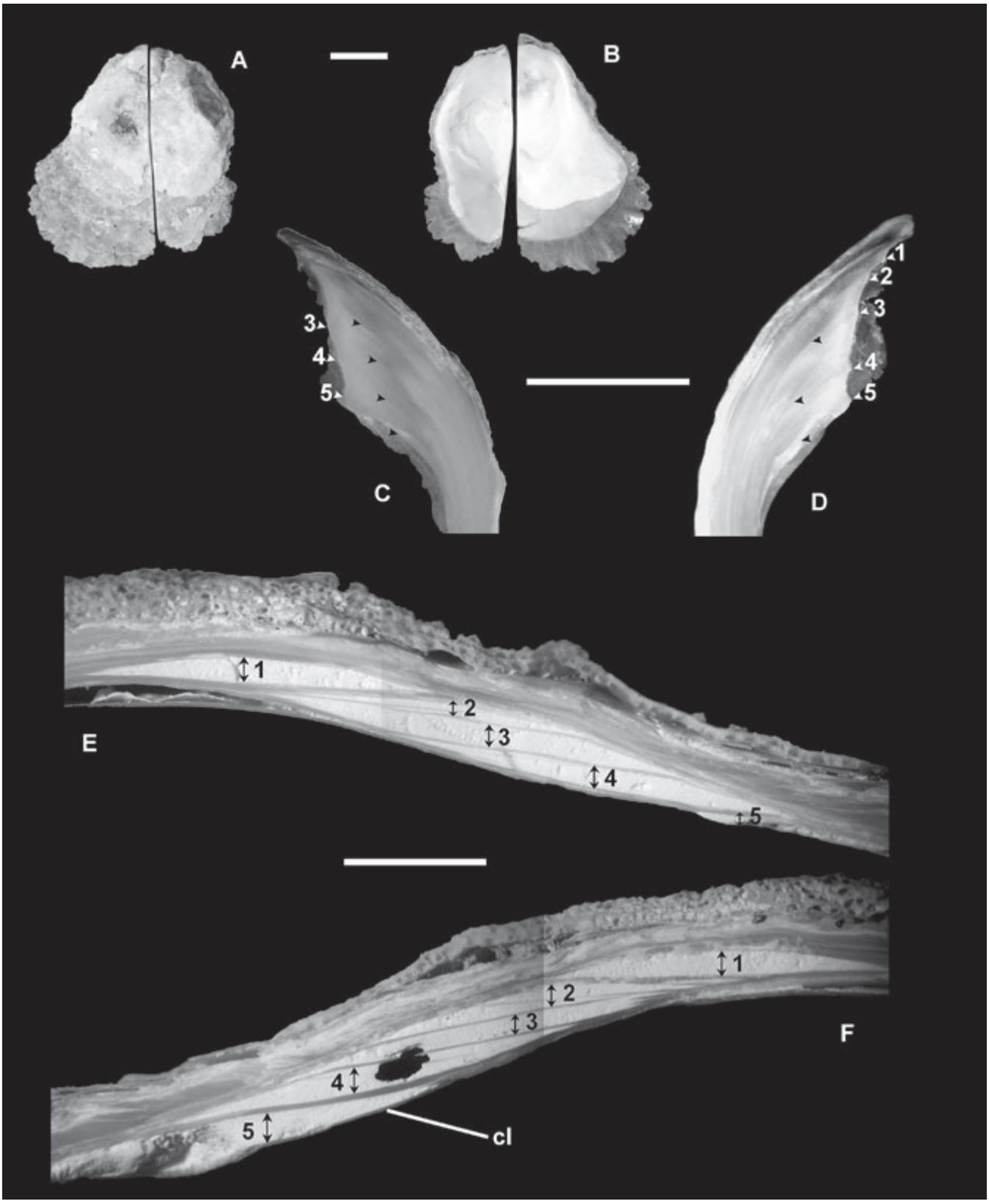

Figure 8A–B Valve L3A', external (A) and internal (B) views, sectioned in two half-valves. **C–D**. Half-valves L3A'*r* (C) and L3A'*l* (D), umbonal section; white numbers/arrows mark the position of annual ligamental ridges, black arrows that of some growth lines. **E–F**. Half-valves L3A'*r* (E) and L3A'*l* (F), mid section; black numbers/arrows mark annual chalky lenses below the muscle scar area. Abbreviations: cl, crystalline calcitic layer. Scale bars: **A–B**=20.0mm; **C–F**=5.0mm.

part of the pit (white arrows), numbered from 3 to 5 (cf. Fig. 8D). Growth lines (black arrows) are quite indistinct, correspond to weak color variations and seem to follow a convex path; their weakness prevents from relating them safely to the ridges. The mid section (Fig. 8E) shows five chalky lenses beneath the muscle scar area, separated by relatively thick crystalline layers; only lenses 3 and 4 appear further subdivided by very thin secondary layers. The youngest lens (5) is only apparently incomplete because of the breaking of the bordering crystalline calcitic layer, and subsequent scraping of the very tender chalky material. The inferred age of this specimen is 5 years.

Half-valve L3A'*l* (Figs 8D, F). In the umbonal area (Fig. 8D), ligamental features are more clearly distinguishable than in L3A'*r*. Five ridges (white arrows) are counted, visible in the section as low protuberances; a secondary fold, not linked to a ridge, occurs between ridges 3 and 4. It is of note that, accordingly with autumn harvesting, the concavity just below ridge 4 is complete, and the deposition of ridge 5 has just begun – thus indicating the cold season growth slowdown. As in the previously described half-valve, growth lines in the section (black arrows) are hardly distinguishable as color variations, in particular as regards those corresponding to ridges 1 and 2; the line related to ridge 5 (lowest arrow) apparently runs through an irregular calcite deposition zone. The mid section (Fig. 8F) exhibits five chalky lenses, just alike half-valve L3A'*r*; in this case, however, lens 5 shows no abrasion and appears completely bounded by a crystalline layer (cl). A small cavitation (bioerosion) occurs between lenses 3 and 4. Morphological evidence confirms that the specimen is presumably 5 years old.

DISCUSSION

Usually, uncertainties in sclerochronological analyses can be minimized by examining a large number of specimens; this proves to be particularly true for oysters, since their sessile habit and extremely irregular growth often generate cracks and cavitations inside the shell, hiding the growth traces (Milner, 2001). As already pointed out, internal growth markings and ligamental ridges have been extensively used in the past for age determination purposes. In the present case, however, only a small number of shells was at hand; the need for a quick (and cheap) age assessment led to evaluate the combined use of different morphological features, in order to obtain a safe estimate of shell ages. Ligamental ridges were often,but not always, clearly detectable on the ligamental pit, and they were retained as the most valuable age indicator. Conversely, umbonal growth lines were obvious only in few cases, taking each ridge as a starting point and following their course toward the ventral side of the valve. In addition, for the first time, the sclerochronological analysis included also internally deposited "chalky" lenses. Actually, in several of the examined half-valves, series of these lenses were noticed just abapical to the adductor muscle insertion area, extending in width throughout the whole shell thickness; they regularly alternate with microcrystalline calcitic layers, often appearing as the continuation of the umbonal growth lines (when distinguishable). Moreover, in most cases (valves L0B', L2B'', L3A') the lenses equal in number the annual ridges counted on the ligamental pit. This led to the assumuption that lens deposition could follow an annual cycle with a cold season interruption, just as with ridges and lines. Most probably, the deposition takes place in the warm season, while the interruption is marked by the appearance of the thick, bounding crystalline layer. These annual lenses are often subdivided into smaller ones by thin secondary crystalline layers, but their overall structure remains clearly detectable. Secondary lenses are considerably smaller and cover only partially the muscle scar area, not extending in the section from the most internal (youngest) crystalline layer to the external layers of the shell. Conversely, annual deposits appear to be considerably thicker, longer in section and deposited more abapically than the preceding ones; above all, they are invariably bordered by relatively thick microcrystalline layers running without interruptions from the internal to the external side of the valve, and not merging into thicker ones unless at the extremities.

Visual sclerochronological analyses based on growth lines or ridges only, in some cases, are likely to underestimate shell ages. In fact, 1) the above cited traces (lines in particular) could be hardly distinguishable, and 2) shell umbo could be incomplete for several ontogenetic reasons (i.e. irregular growth, partial dissolution, shell

damaging during mollusc's life span, occurring of internal cavitations). The additional use of chalky deposits may considerably reduce this uncertainty, since they are much more clearly recognizable and extended on a wider (i.e. more easily intercepted during valve cutting) portion of the shell. They appear as a definitely easy-to-use feature, sometimes detectable just with the naked eye, for a quick age assessment.

The proposed combined visual examination yielded estimated ages roughly agreeing with shell dimensions as known from some literature (cf. Richardson *et al*., 1993; Walne, 1958). Nevertheless, shell dimensions alone cannot be retained as a reliable age proxy. Actually, the whole life cycle (including both settlement and growth) of *O. edulis* appears to be strictly dependent on genetic factors, as well as on several environmental parameters like water temperature, food availability, tidal exposure, and impact of parasites (cf. Robert, Borel, Pichot & Trut, 1991; Ruiz, Martinez, Mosquera, Abad & Sánchez, 1992; Walne, 1958).

This is supposed to lead to differential growth rates even between nearby localities. In order to support this hypothesis, a Von Bertalanffy (VB) growth curve ('L' in Fig. 2) was drawn on the basis of age-length data of our specimens. This methodology has been extensively adopted, particularly in recent years, in studying growth characteristics of several different bivalve genera (see for example the recent papers by Fiori & Morsan, 2004 on *Mesodesma*; Garcia-March, Marquez-Aliaga, Wang, Surge & Kersting, 2011 on *Pinna*; Harding & Mann, 2006 on *Crassostrea*; Peharda, Richardson, Onofri, Bratoš & Crnčević, 2002 on *Arca*).

The Livorno growth curve in Fig. 2 shows a mean height of 38.6mm for 1-year old, 60.1mm for 2-years old, and 72mm for 3-years old specimens; subsequently, growth rate rapidly decreases. A size very close to the asymptotic one (87mm) is reached from ten years onward.

Noticeable differences are noted when comparing these data with the ones resulting from other VB growth curves built on European *O. edulis* stocks (Fig. 2). Oysters from the Central Adriatic Sea (off Conero cape nearby Ancona; Fabi, Fiorentini & Giannini, 1989) attain a mean height of about 67mm in their second year, though the VB asymptotic height is only 77mm (curve 'A' in Fig. 2).

Specimens from the Northeastern Atlantic exhibit an even greater discrepancy. *O. edulis* from Hampshire waters (S England; Rodhouse, 1978) reached a 60mm size after 5 years, but seem to follow a long-lasting growth cycle attaining a maximum height of about 100mm in 15 to 20 years (curve 'H' in Fig. 2). Moreover, Richardson *et al*. (1993) report a marked variability between stocks not so far from each other: specimens from SE England (curve 'B' in Fig. 2) coast show a more rapid growth and a greater asymptotic height than their counterparts living on SW coast (curve 'F' in Fig. 2), reaching 60mm in 2–3 years rather than in 5 years and a theoretical maximum of 93mm against 72–80mm, respectively.

Commonly, sclerochronological analyses include age determination of shells and other mineralized parts for the reconstruction of long-term curves that proved to be very useful for either stratigraphic, (palaeo)ecological and palaeoclimatic scopes (see, for example, Butler, Richardson, Scourse, Wanamaker, Shammon & Bennell, 2010; Gröcke & Gillikin, 2008; Marchitto *et al*., 2000). Oysters appear unsuitable for such scopes, due to their short mean lifetime and the difficulty in overlapping their sclerochronological record back in time. Yet, oyster larvae possess a quick settling capability, becoming ready to settle on available hard substrates within few days after their release (see for example the experiments by Davis & Calabrese, 1969 and Jonsson, Berntsson, André & Wängberg, 1999); the latter occurs 6–10 days after spawning (cf. Loosanoff, Davis & Chanley, 1966) which, being a temperature-dependent process, normally takes place in the warm season, from mid spring to late summer (cf. Milner, 2001; Ruiz *et al*., 1992). Consequently, a hitherto virtually unexplored application of sclerochronological results can be hypothesized, at least for areas hosting consistent wild oyster populations, i.e. the precise definition of the time in which the substrate they are found attached to became available for settling. This could prove to be very useful in cases where the substrate is a human artifact placed on record as evidence in legal proceedings or involved in a technical survey. In fact, oyster age assessment can help in determining exactly when the anthropogenic substrate was either intentionally placed or accidentally dropped to the seafloor, or exhumed from bottom sediments to the seafloor/water interface.

ACKNOWLEDGEMENTS

The research was entirely funded by internal funds (FAR) of the Milano-Bicocca University. The paper benefited from critical reading by Daniela Basso (University of Milano-Bicocca). We thank Sergio Andò (University of Milano-Bicocca) for assistance during valves cutting operations. We are very grateful to suggestions offered by the anonymous referees in the formal review of the paper.

REFERENCES

BUTLER PG, RICHARDSON CA, SCOURSE JD, WANAMAKER AD JR, SHAMMON TM & BENNELL JD 2010 Marine climate in the Irish Sea: analysis of a 489-year marine master chronology derived from growth increments in the shell of the clam *Arctica islandica Quaternary Science Reviews* **29**: 1614–1632.

CHINZEI K 1986 Shell structure, growth, and functional morphology of an elongate Cretaceous oyster *Palaeontology* **29** (1): 139–154.

CHINZEI K 1995 Adaptive significance of the lightweight shell structure in soft bottom oysters *Neues Jahrbuch für Geologie und Paläontologie* **195**: 217–227.

CLAUSEN CD 1974 An evaluation of the use of growth lines in geochronology, geophysics and Paleoecology *Origins* **1** (2): 58–66.

DAUPHIN Y, BALL AD, CASTILLO-MICHEL H, CHEVALLARD C, CUIF J–P, Farre B, Pouvreau S & Salomé M 2013 *In situ* distribution and characterization of the organic content of the oyster shell *Crassostrea gigas* (Mollusca, Bivalvia) *Micron* **44**: 373–383.

DAVIS HC & CALABRESE A 1969 Survival and growth of larvae of the European oyster (*Ostrea edulis* L.) at different temperatures *The Biological Bulletin* **136** (2): 193–199.

FABI G, FIORENTINI L & GIANNINI S 1989 Experimental shellfish culture on an artificial reef in the Adriatic Sea *Bulletin of Marine Science* **44** (2): 923–933.

FIORI SM & MORSÁN EM 2004 Age and individual growth of *Mesodesma mactroides* (Bivalvia) in the southernmost range of its distribution *ICES Journal of Marine Science* **61**: 1253–1259.

GARCIA-MARCH JR, MARQUEZ-ALIAGA A, WANG Y–G, Surge D & Kersting DK 2011 Study of *Pinna nobilis* growth from inner record: How biased are posterior adductor muscle scars estimates? *Journal of Experimental Marine Biology and Ecology* **407**: 337–344.

GRÖCKE DR & GILLIKIN DP 2008 Advances in mollusc sclerochronology and sclerochemistry: tools for understanding climate and environment *Geo-Marine Letters* **28**: 265–268.

HARDING JM & MANN R 2006 Age and growth of wild suminoe (*Crassostrea ariakensis*, Fugita 1913) and Pacific (*C. gigas*, Thunberg 1793) oysters from Laizhou Bay, China *Journal of Shellfish Research* **25** (1): 73–82.

JONSSON PR, BERNTSSON KM, ANDRÉ C & WÄNGBERG S–Å 1999 Larval growth and settlement of the European oyster (*Ostrea edulis*) as a function of food quality measured as fatty acid composition *Marine Biology* **134**: 559–570.

KIRBY MX 2001 Differences in growth rates and environment between Tertiary and Quaternary *Crassostrea* oysters *Paleobiology* **27** (1): 84–103.

KIRBY MX, SONIAT TM & SPERO HJ 1998 Stable isotope sclerochronology of Pleistocene and Recent oyster shells (*Crassostrea virginica*) *Palaios* **13** (6): 560–569.

KOMATSU T, CHINZEI K, ZAKHERA MS & MATSUOKA H 2002 Jurassic soft-bottom oyster *Crassostrea* from Japan *Palaeontology* **45** (6): 1037–1048.

LOOSANOFF VL, DAVIS HC & CHANLEY PE 1966 Dimensions and shapes of larvae of some marine mollusks *Malacologia* **4** (2): 351–435.

MACDONALD J, FREER A & CUSACK M 2010 Alignment of Crystallographic c-Axis throughout the Four Distinct Microstructural Layers of the Oyster *Crassostrea gigas Crystal growth & Design* **10** (3): 1243–1246.

MARCHITTO TM, JONES GA, GOODFRIEND GA & WEIDMAN CR 2000 Precise Temporal Correlation of Holocene Mollusk Shells Using Sclerochronology *Quaternary Research* **53**: 236–246.

MILNER N 2001 At the Cutting Edge: Using Thin Sectioning to Determine Season of Death of the European Oyster, *Ostrea edulis Journal of Archaeological Science* **28**: 861–873.

PEHARDA M, RICHARDSON CA, ONOFRI V, BRATOŠ A & CRNČEVIĆ M 2002 Age and growth of the bivalve *Arca noae* L. in the Croatian Adriatic Sea *Journal of Molluscan Studies* **68**: 307–310.

RICHARDSON CA, COLLIS SA, EKARATNE K, DARE P & KEY D 1993 The age determination and growth rate of the European flat oyster, *Ostrea edulis*, in British waters determined from acetate peels of umbo growth lines *Journal of Marine Science: Journal du Conseil* **50** (4): 493–500.

ROBERT R, BOREL M, PICHOT Y & TRUT G 1991 Growth and mortality of the European oyster *Ostrea edulis* in the Bay of Arcachon (France) *Aquatic Living Resources* **4**: 265–274.

RODHOUSE PG 1978 Energy transformations by the oyster *Ostrea edulis* L. in a temperate estuary *Journal of Experimental Marine Biology and Ecology* **34**: 1–22.

RUIZ C, MARTINEZ D, MOSQUERA G, ABAD M & SÁNCHEZ JL 1992 Seasonal variations in condition, reproductive activity and biochemical composition of the flat oyster, *Ostrea edulis*, from San Cibran (Galicia, Spain) *Marine Biology* **112**: 67–74.

SPARRE P & VENEMA SC 1998 *Introduction to tropical fish stock assessment. Part I: manual* FAO Fisheries Technical Paper **306**/1 (rev. 2), 407 pp.

TOLAND H, PERKINS B, PEARCE N, KEENAR F & LENG MJ 2000 A study of sclerochronology by laser ablation ICP-MS *Journal of Analytical Atomic Spectrometry* **15**: 1143–1148.

WALNE PR 1958 Growth of oysters (*Ostrea edulis* L.) *Journal of the Marine Biological Association of the U.K.* **37**: 591–602.